11th International Conference on Vibration Problems
Z. Dimitrovová *et.al.* (eds.)
Lisbon, Portugal, 9–12 September 2013

CONTROLLING THE NATURE OF BIFURCATION IN FRICTION-INDUCED VIBRATIONS WITH A DYNAMIC (LUGRE) FRICTION MODEL BY DELAYED POSITION FEEDBACK

Ashesh Saha[1], Pankaj Wahi*[2]

[1]Mechanical Engineering Department, Indian Institute of Technology-Kanpur
asheshjgec@gmail.com

[2]Mechanical Engineering Department, Indian Institute of Technology-Kanpur
wahi@iitk.ac.in

Keywords: Friction-induced vibrations, Time-delayed feedback, Dynamic friction, Bifurcation control.

Abstract. *We analyse the effect of time-delayed position feedback in controlling friction-induced vibrations of a single degree-of-freedom spring-mass-damper system on a moving belt. The friction force is modeled by a dynamic (LuGre) friction model. The control force is applied in a direction normal to the friction force. Linear stability analysis shows that the stability of the steady-state changes via a Hopf bifurcation. Numerical analysis of the full nonlinear equations reveals the possibility of changing the nature of the bifurcation from subcritical to supercritical using the linear control force employed in our study. Detailed numerical studies using a continuation scheme shows an interesting range of control parameters for which the steady-state is stable for low and high belt velocities and unstable for the intermediate ones. Interestingly, this phenomena is observed only for those control parameters for which the bifurcation is supercritical in nature. In particular, there are combinations of control parameters for which the range of intermediate belt velocities corresponding to vibrations is small and only pure slipping motions are present because of the supercritical nature of the bifurcation. Hence, these set of control parameters are ideal for practical implementation since the non-smooth stick-slip motions are avoided.*

1 INTRODUCTION

In this paper, we explore the efficacy of a linear time-delayed position feedback in quenching friction-induced vibrations along with changing the nature of bifurcation from subcritical to supercritical. For simplicity of analysis, we consider a single-degree-of-freedom friction-induced system consisting of a spring-mass-damper system with the mass resting on a belt moving with constant velocity. The control force is applied in a direction normal to the friction force.

Friction-induced vibrations is a type of self-excited oscillations [1] in which the system of interest is in frictional contact with another system which is driven by a power source. Friction force then transfers energy from the drive system to the system of interest leading to instabilities. This type of vibrations is frequently encountered in many engineering systems. Some typical examples are: brake-squeal, train curve squeal, clutch chatter, machine-tool chatter, friction-induced vibrations in robotic joints and friction-induced vibrations in lead screw drives. Due to their detrimental effects like high levels of noise, excessive wear of components, surface damage and fatigue failure, these unwanted vibrations should be controlled in engineering systems.

The three widely studied instability mechanisms developed in the literature to investigate the friction-induced vibrations are: (i) instability due to the presence of an effective negative damping in the governing equations of motion [2, 3, 4], (ii) the mode coupling instability [5, 6], and (iii) the sprag-slip instability [7, 8]. The negative damping in the system appears due to the drooping characteristic of the friction force in the low relative velocity regime (also known as the Stribeck effect). The last two instability mechanisms, however, do not require variable friction coefficient to induce vibrations. We will only consider the instability due to the Stribeck effect of the friction force in this paper to study the control of friction-induced vibrations by time-delayed position feedback.

Friction modeling is an inherent part of the study of frictional instability. There is a vast literature on the development of different friction models that can describe different experimentally observed friction phenomena [2, 3, 4, 9, 10, 11, 12, 13, 14]. Depending on the functional forms, the friction models can be divided into three categories : (i) static friction models [2, 3, 4], (ii) dynamic friction models [9, 10, 11] and (iii) acceleration-dependent friction models [12, 13, 14]. Coulomb friction model and Stribeck friction models, in which the friction force depends on the relative velocity of the contacting surfaces, fall under the category of static friction models. The static friction models cannot describe the hysteretic effects of friction and so, dynamic friction models and acceleration-dependent friction models are developed.

In our previous works [15, 16, 17], we have mainly considered Stribeck friction models. However, hysteretic effects of friction are also important for complete description of friction phenomena and have been observed experimentally under unsteady conditions (especially periodic vibrations) where the relative velocity oscillates [10, 13, 14, 18, 19]. In this paper, we consider the LuGre friction model proposed by Canudas de Wit *et al.* [10] which is a widely used dynamic friction model. The bifurcation of the uncontrolled friction-induced oscillation system with the LuGre friction model is found to be subcritical in nature [16, 20]. This type of bifurcation is generally known as hard (or dangerous) in a sense that the steady-state of the system might become unstable due to a definite perturbation of a system parameter near the stability boundary resulting in a large amplitude vibrations. In contrast, supercritical bifurcation is sometimes called soft (or safe) in engineering literature due to the fact that this type of bifurcation guarantees global stability in the linearly stable regime and small amplitude vibrations when the stability boundaries are crossed preventing detrimental damage to the structure. Hence, supercritical bifurcations are more desirable than the subcritical bifurcations. In this

present study, we explore the possibility of achieving supercritical bifurcation using an appropriate control strategy.

Several control strategies (both passive and active) have been developed in the literature to attenuate or completely quench friction-induced vibrations [4, 15, 16, 17, 20, 21, 22, 23]. Controlling these vibrations due to the drooping characteristics by using a traditional PID controller requires a derivative component. However, a time-delayed controller only needs a position feedback to quench friction-induced vibrations completely [16, 22, 23, 15, 17] making it a popular choice among researchers. In this work, we apply linear time-delayed position feedback in a direction normal to the friction force to increase the stable regions as well as to control the nature of associated bifurcation. The reason that we achieve supercritical bifurcation is due to the fact that the control force couples with the inherent nonlinearities of the friction force and produces new nonlinear terms. The feedback controller is of the same form as that discussed in [15, 16, 17, 23].

The rest of the paper is organised as follows. We introduce the mathematical model of the system with the LuGre friction model in Section 2 with control force applied in a direction normal to the friction force. Linear stability analysis is performed in Section 3 to obtain the stability boundaries separating the linearly stable and unstable equilibriums. Various results are discussed in detail in Section 4. Finally, some conclusions are drawn in Section 5.

2 THE MATHEMATICAL MODEL

In this present study on the control of friction-induced oscillations, we consider a simplified model consisting of a spring-mass-damper system with the mass resting on a friction belt moving with a constant velocity. The schematic representation of the corresponding physical model is shown in Fig. 1 in which N_0^* is the normal load (including the weight $M\,g$ of the oscillator block) in the absence of control force and F_c^* is the control force. The control force is applied in a direction normal to the friction force which we call as the 'normal control force' for simplicity.
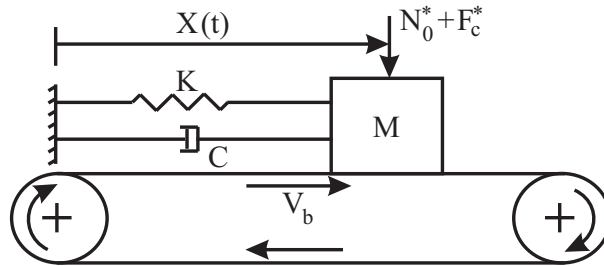

Figure 1: Damped harmonic oscillator on a moving belt as a model for friction-driven vibrations with normal control force.

The governing equation for this system with normal control force is given by

$$M\,\frac{d^2 X}{dt^2} + C\,\frac{dX}{dt} + K\,X = (N_0^* + F_c^*)\,f\,(V_r)\,,\tag{1}$$

where N_0^* is the total normal load acting on the slider in the absence of the control force, F_c^* is the control force and $f\,(V_r)$ is the friction function (friction force per unit of normal load). We will use time-delayed control force of the following form [15, 16, 17, 23]:

$$F_c^* = K_{c1}^*\,(X\,(t - T_1^*) - X(t))\,.\tag{2}$$

3

where K_{c1}^* is the control gain and T_1^* is the time-delay. Using the characteristic time scale fixed by $\omega_0 = \sqrt{K/M}$ and the characteristic length fixed by $x_0 = g/\omega_0^2$, we obtain the non-dimensional equation of motion as

$$x'' + 2\,\xi\,x' + x = (N_0 + K_{c1}\,(x\,(\tau - T_1) - x\,(\tau)))\,f\,(v_r)\,, \tag{3}$$

where primes denote derivative with respect to the non-dimensional time $\tau = \omega_0\,t$. The other non-dimensional quantities are

$x = \dfrac{X}{x_0}$, $v_b = \dfrac{V_b}{\omega_0\,x_0}$, $v_r = v_b - x'$, $\xi = \dfrac{C}{2\,M\,\omega_0}$, $N_0 = \dfrac{N_0^*}{M\,\omega_0^2\,x_0}$, $K_{c1} = \dfrac{K_{c1}^*}{M\,\omega_0^2}$, $T_1 = \omega_0\,T_1^*$.

We represent the friction function $f\,(v_r)$ by the LuGre friction model [10] which is one of the most widely used form of a dynamic friction model and it includes more complicated physical phenomenon like hysteresis associated with friction. In this model, the asperities in the contact surfaces are considered as elastic spring like bristles with damping and the microscopic degrees of freedom associated with the bristle deflections are used to define the friction force. The total friction force in the LuGre friction model is considered to be a summation of the average force associated with the deflection of the bristles and a viscous term proportional to the relative velocity between the surfaces in contact. The friction function is accordingly given by

$$f\,(v_r) = \sigma_0\,\hat{z} + \sigma_1\,\frac{d\hat{z}}{d\tau} + \sigma_2\,v_r, \tag{4}$$

where $\hat{z}$ is the average bristle deflection, σ_0 is the bristle stiffness, σ_1 is the bristle damping and σ_2 is the viscous component of the frictional force. The equation governing the evolution of the average bristle deflection (see [10]) is

$$\frac{d\hat{z}}{d\tau} = v_r\left(1 - \frac{\sigma_0\,\hat{z}}{g\,(v_r)}\,\mathrm{sgn}(v_r)\right). \tag{5}$$

The function $g\,(v_r)$ in the above equation determines the stribeck effect (or the drooping characteristic) and it is represented as

$$g\,(v_r) = \mu_k + \Delta\mu\,\mathrm{e}^{-\left(\frac{v_r}{v_s}\right)^2}, \tag{6}$$

where v_s is the stribeck velocity which is the relative velocity at the transition from microslip (stick) to macroslip. Equations (3) to (6) describe the complete equations of motion for our system which can be written compactly in the state-space form as

$$
\begin{aligned}
x' &= u\,, \\
u' &= -2\,\xi\,u - x + (N_0 + K_{c1}\,((x)_{T_1} - x))\left(\sigma_0\,\hat{z} + \sigma_1\,\frac{d\hat{z}}{d\tau} + \sigma_2\,v_r\right), \\
\hat{z}' &= v_r\left(1 - \frac{\sigma_0\,\hat{z}}{g\,(v_r)}\,\mathrm{sgn}(v_r)\right),
\end{aligned}
\tag{7}
$$

where $v_r = v_b - x'$.

3 LINEAR STABILITY ANALYSIS

We first find the fixed points of the system given by eqn. (7) by setting $(x' = u' = \hat{z}' = 0)$ as $x_s = N_0\,(g\,(v_b) + \sigma_2\,v_b)$, $u_s = 0$ and $\hat{z}_s = -\dfrac{g\,(v_b)}{\sigma_0}$. Linearizing eqn. (7) about these fixed points, we get

$$\widetilde{\mathbf{x}}' = \mathbf{L}\,\widetilde{\mathbf{x}} + \mathbf{R}\,(\widetilde{\mathbf{x}})_{T_1}\,, \tag{8}$$

4

where $\widetilde{\mathbf{x}} = (x - x_s, u - u_s, \hat{z} - \hat{z}_s)^T$ and the matrices $\mathbf{L}$ and $\mathbf{R}$ are

$$\mathbf{L} = \begin{bmatrix} 0 & 1 & 0 \\ -1 - K_{c1}\left(g\left(v_b\right) + \sigma_2 v_b\right) & -2\,\xi - N_0\left(\frac{\sigma_1\,v_b\,g'(v_b)}{g(v_b)} + \sigma_2\right) & \sigma_0\,N_0\left(1 - \frac{\sigma_1\,v_b}{g(v_b)}\right) \\ 0 & -\frac{v_b\,g'(v_b)}{g(v_b)} & \frac{\sigma_0\,v_b}{g(v_b)} \end{bmatrix} \quad (9)$$

and

$$\mathbf{R} = \begin{bmatrix} 0 & 0 & 0 \\ K_{c1}\left(g\left(v_b\right) + \sigma_2 v_b\right) & 0 & 0 \\ 0 & 0 & 0 \end{bmatrix}. \quad (10)$$

Substituting $\widetilde{\mathbf{x}} = \widetilde{\mathbf{c}}\,\mathrm{e}^{s\,\tau}$ in eqn. (8), we obtain the characteristic equation

$$\det(\mathbf{L} + \mathbf{R}\,\mathrm{e}^{-s\,\tau} - s\,\mathbf{I}) = 0, \quad (11)$$

where $\mathbf{I}$ is the identity matrix. Substitution of $\mathbf{L}$ and $\mathbf{R}$ from eqns. (9) and (10) in eqn. (11) results in

$$s^3 + \alpha_2\,s^2 + \alpha_1\,s + a_0 + b_0\,K_{c1}\left(s + a_0\right)\left(1 - \mathrm{e}^{-s\,T_1}\right) = 0, \quad (12)$$

where $\alpha_2 = 2\,\xi + a_0 + N_0\left(\sigma_2 + a_0\frac{\sigma_1}{\sigma_0}g'\left(v_b\right)\right)$, $\alpha_1 = 1 + 2\,\xi\,a_0 + a_0\,N_0\left(\sigma_2 + g'\left(v_b\right)\right)$, $a_0 = \frac{\sigma_0\,v_b}{g\left(v_b\right)}$ and $b_0 = g\left(v_b\right) + \sigma_2\,v_b$. At the stability boundary corresponding to the Hopf bifurcation, we have $s = j\,\omega$. Substituting this in eqn. (12) and separating the real and imaginary parts, we get

$$\omega\,b_0\,K_{c1}\,\sin(\omega\,T_1) + a_0\,b_0\,K_{c1}\,\cos(\omega\,T_1) = a_0 + a_0\,b_0\,K_{c1} - \alpha_2\,\omega^2, \quad (13)$$
$$a_0\,b_0\,K_{c1}\,\sin(\omega\,T_1) - \omega\,b_0\,K_{c1}\,\cos(\omega\,T_1) = \omega^3 - \alpha_1\,\omega. \quad (14)$$

The critical values of K_{c1} and T_1 are obtained by solving eqns. (13) and (14) as

$$\begin{aligned} K_{c1o} &= \frac{\omega^6 + \left(\alpha_2^2 - 2\,\alpha_1\right)\omega^4 + \left(\alpha_1^2 - 2\,a_0\,\alpha_2\right)\omega^2 + a_0^2}{2\,b_0\left(\omega^4 - \left(\alpha_1 - a_0\,\alpha_2\right)\omega^2 - a_0^2\right)}, \\ T_{1o} &= \frac{2}{\omega}\left[\tan^{-1}\left(\frac{\omega^4 + \left(a_0\,\alpha_2 - \alpha_1\right)\omega^2 - a_0^2}{\left(a_0 - \alpha_2\right)\omega^3 - \left(a_0\,\alpha_1 + \alpha_2\right)\omega}\right) + 2\,i\,\pi\right] \quad \forall i = 0, 1, 2, \ldots, \infty. \end{aligned} \quad (15)$$

4 RESULTS AND DISCUSSIONS

The stability boundaries in the plane of the control parameters for different belt velocities v_b and normal load N_0 are shown in Fig. 2 using eqn. (15). The stable region increases with an increase in the belt velocity v_b and a decrease in the pre-normal load N_0.

Figure 3 shows the critical belt velocity v_{bo} corresponding to the Hopf bifurcation point as a function of the time-delay T_1 for different values of control gains K_{c1}. Regions A and B in Fig. 3 are stable and unstable equilibrium regions, respectively. It is observed from Fig. 3 that for some set of control parameters, especially corresponding to small time-delays, there exists two values of v_{bo}; one on the higher side and the other in the lower side. For convenience, we call these values of v_{bo} as $(v_{bo})_h$ and $(v_{bo})_l$, respectively. Hence, we expect two Hopf bifurcation points in the bifurcation diagram for these set of control parameters. It is also observed from Fig. 3 that the critical belt velocity $(v_{bo})_h$ first decreases with the increase of time-delay T_1, reaches a minimum for a certain T_1 and then increases again. Beyond a particular value of T_1, the critical belt velocity for the controlled system becomes higher than that for the uncontrolled
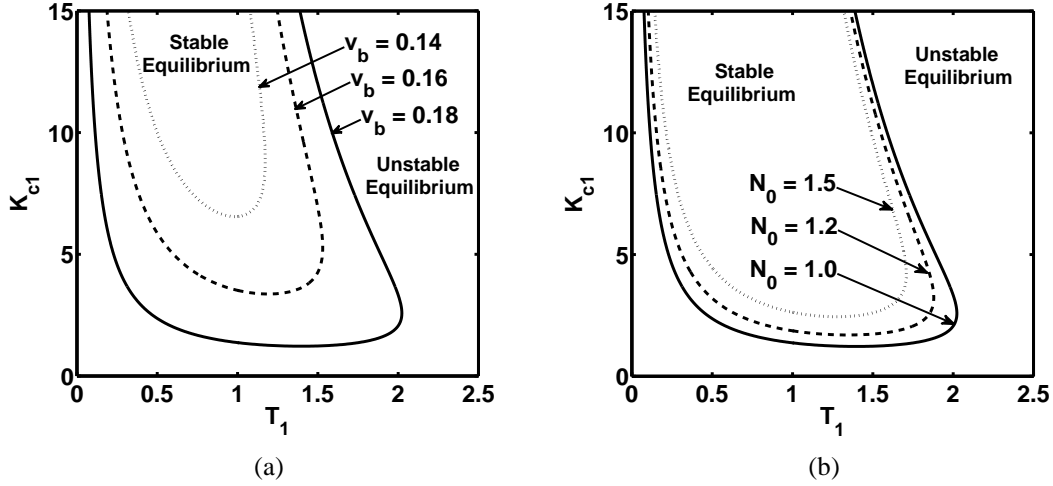
Figure 2: Stability boundaries for normal control force with LuGre friction model. Parameters: $\mu_s = 0.3$, $\mu_k = 0.1$, $v_s = 0.1$, $\xi = 0.05$, $\sigma_0 = 100$, $\sigma_1 = 10$, $\sigma_2 = 0.05$, (a) $N_0 = 1$, (b) $v_b = 0.18$.
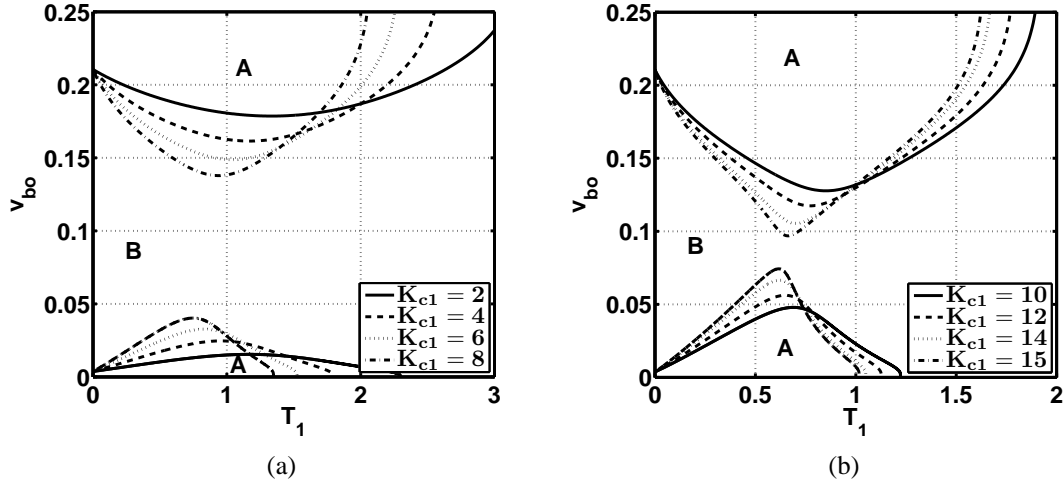

Figure 3: Time-delay vs critical belt velocity for different control gains. Region A: stable equilibrium, region B: unstable equilibrium. Parameters: $\mu_s = 0.3$, $\mu_k = 0.1$, $v_s = 0.1$, $\xi = 0.05$, $\sigma_0 = 100$, $\sigma_1 = 10$, $\sigma_2 = 0$, $N_0 = 1$.

system which is certainly undesirable. A completely opposite situation occurs for $(v_{bo})_l$; it first increases with the increase of T_1, reaches a maximum and then decreases again till it vanishes for a particular value of T_1. The minimum value of $(v_{bo})_h$ and the maximum value of $(v_{bo})_l$, however, do not occur for the same value of T_1. Again, we observe from Fig. 3 that the magnitude of $(v_{bo})_h$ decreases with the increasing values of control gain K_{c1} and the magnitude of $(v_{bo})_l$ increases with the increasing values of control gain K_{c1}. The two critical belt velocities $(v_{bo})_h$ and $(v_{bo})_l$ come very close to each other for a very high value of control gain K_{c1}. These observations will be more clear when we plot the bifurcation diagrams later in this section for different set of control parameters.

Having established the effectiveness of the linear normal control force in quenching vibrations for the LuGre friction model, we need to study its effect on the nature of the bifurcation. In that direction, we present the bifurcation diagrams generated numerically using the DDE-BIFTOOL [24] for two typical set of control parameters, one belonging to the subcritical regime ($K_{c1} = 1$ with $T_1 = 1$) and the other to the supercritical regime ($K_{c1} = 7$ with $T_1 = 1$) in Fig. 4. In the bifurcation diagrams, the variation of the amplitudes of the limit cycles are
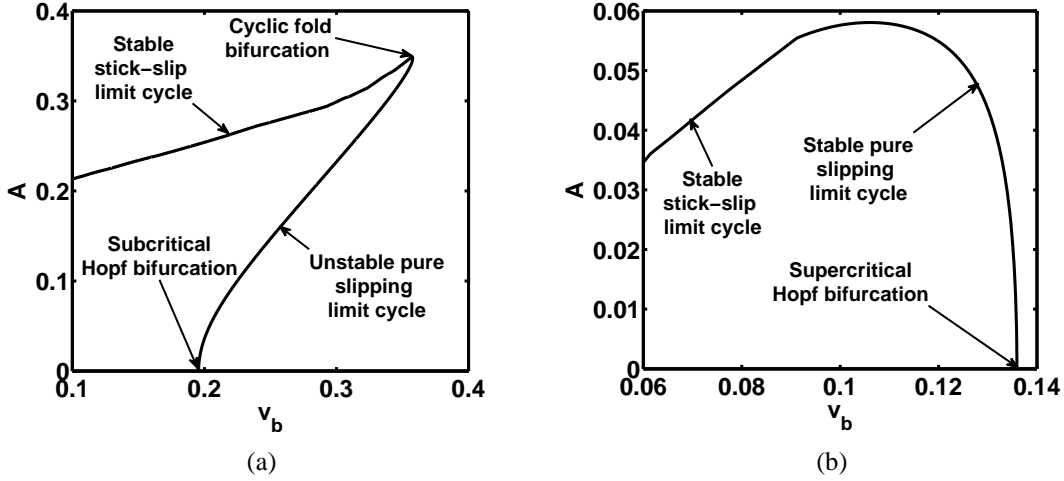
Figure 4: Bifurcation diagrams with v_b as the bifurcation parameter. Parameters: $\mu_s = 0.3$, $\mu_k = 0.1$, $v_s = 0.1$, $\xi = 0.05$, $N_0 = 1$, $\sigma_0 = 100$, $\sigma_1 = 10$, $\sigma_2 = 0$, $T_1 = 0.75$, (a) $K_{c1} = 1$, (b) $K_{c1} = 9$.

plotted against the belt velocity v_b. It is observed from Fig. 4 that for lower values of the control gain K_{c1} the bifurcation is subcritical in nature while when the control gain is increased above a certain critical value, the nature of the bifurcation becomes supercritical.

To show the transition of bifurcation from subcritical to supercritical for increasing value of control gain K_{c1}, some more bifurcation diagrams for different values of K_{c1} (for fixed value of $T_1 = 0.75$) are plotted in Fig. 5. As expected, the critical belt velocity $(v_{bo})_h$ decreases with increasing values of K_{c1}. An interesting phenomena could be observed from the bifurcation diagrams in Figs. 5(a) and (b). We observe from these bifurcation diagrams that for some intermediate K_{c1} values the unstable pure slipping limit cycles resulting from the subcritical Hopf bifurcation stabilizes to result in stable pure-slipping limit cycles at the turning point (fold bifurcation point). This phenomena could be recognized clearly from the bifurcation diagrams for $K_{c1} = 4$ and $K_{c1} = 5$. It is observed from Fig. 5(b) that supercritical bifurcation is achieved for a control gain of $K_{c1} = 8$ and the nature of bifurcation is subcritical for all control gains lower than this value. Figure 5(c) shows supercritical bifurcations obtained for control gains $K_{c1} = 8$, 9, 10 and 11, respectively. Both the critical belt velocities $(v_{bo})_h$ and $(v_{bo})_l$ for a particular set of control parameters could be observed from these bifurcation diagrams. However, we have not found $(v_{bo})_l$ from numerical simulation while the bifurcation is subcritical in nature. As discussed earlier and as shown in Fig. 3, the critical belt velocities $(v_{bo})_h$ and $(v_{bo})_l$ approach each other for higher values of K_{c1} and the equilibrium is globally stable for belt velocities $v_b > (v_{bo})_h$ and $v_b < (v_{bo})_l$.

To investigate the effect of the control force on the system vibrations, time-history of the displacement and phase-plane plots of the system before and after the application of the control force with varying control gains are shown in Figs. 6(a) and (b), respectively. The belt velocity chosen for obtaining these figures is $v_b = 0.18$ for which an unstable pure slipping limit cycle coexists with a stable pure slipping limit cycle when the control gain is $K_{c1} = 4$ (see Fig. 5(a)). We first obtain the time-response in Fig. 6(a) for the non-dimensional time span $\tau = 0 - 150$ without the application of the control force (uncontrolled system). At time $\tau = 150$ the control force with gain $K_{c1} = 2$ is applied leading to a reduced amplitude of vibration. The control gain is then increased to $K_{c1} = 4$ at $\tau = 300$, to $K_{c1} = 4.2$ at $\tau = 450$ and to $K_{c1} = 5$ at $\tau = 600$. In all the aforementioned cases, the time-delay is fixed to $T_1 = 0.75$. Every time, the amplitude of vibration decreases with the increase of control gain and ultimately, the vibration ceases to
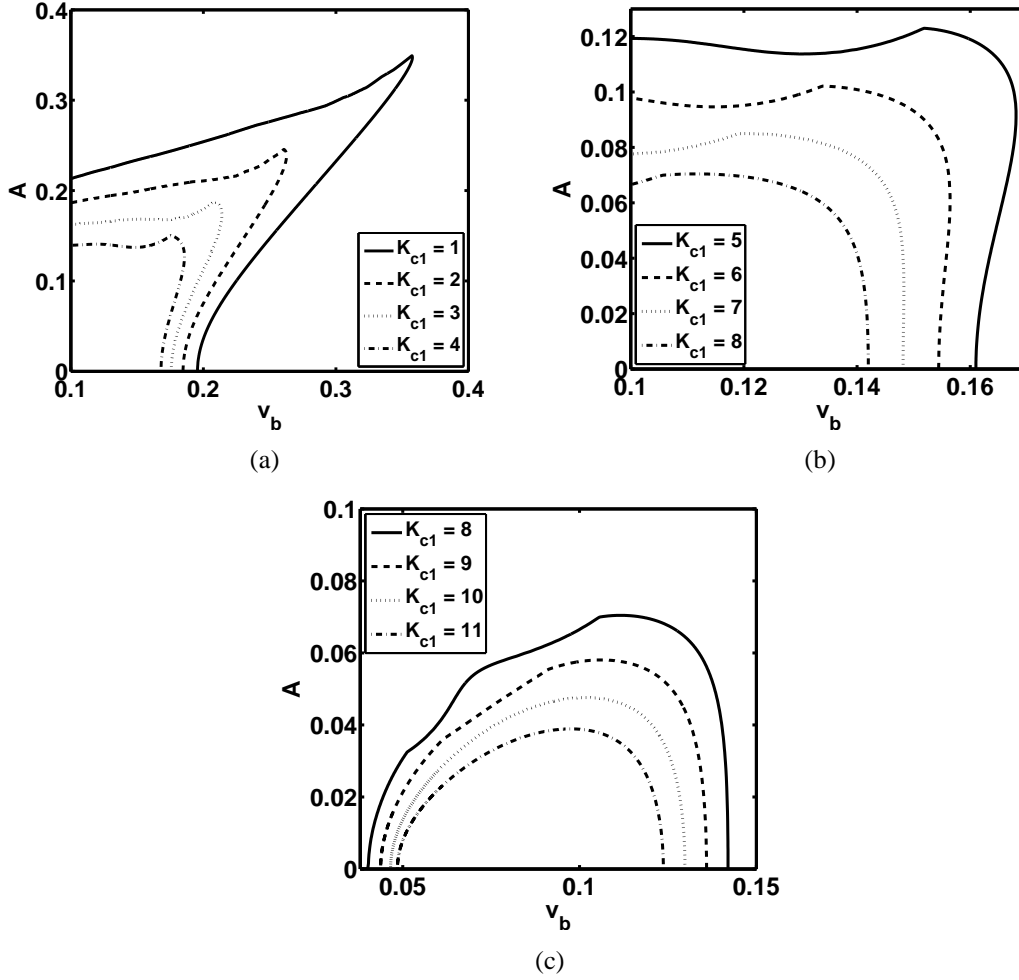
(a)

(b)

(c)

Figure 5: Bifurcation diagrams with v_b as the bifurcation parameter. Parameters: $\mu_s = 0.3$, $\mu_k = 0.1$, $v_s = 0.1$, $\xi = 0.05$, $N_0 = 1$, $\sigma_0 = 100$, $\sigma_1 = 10$, $\sigma_2 = 0$, $T_1 = 0.75$.
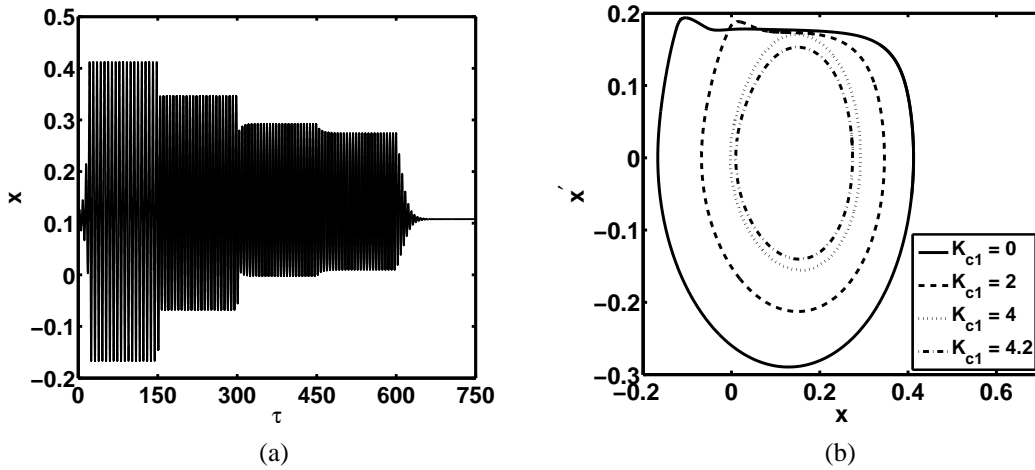

(a)

(b)

Figure 6: (a) Time-displacement response. Control gain K_{c1} for $(\tau = 0 - 150)$: 0, $(\tau = 150 - 300)$: 2, $(\tau = 300 - 450)$: 4, $(\tau = 450 - 600)$: 4.2, $(\tau = 600 - 750)$: 5. (b) Phase-plane plots. Other parameters: $v_b = 0.18$, $\mu_s = 0.3$, $\mu_k = 0.1$, $v_s = 0.1$, $\xi = 0.05$, $N_0 = 1$, $\sigma_0 = 100$, $\sigma_1 = 10$, $\sigma_2 = 0$, $T_1 = 0.75$.

8

exist for $K_{c1} = 5$. The phase-plane plots in Fig. 6(b) show that the vibration is stick-slip in nature for the uncontrolled system and for the controlled system with $K_{c1} = 2$. The limit cycles become pure slipping in nature for control gains $K_{c1} = 4$ and $K_{c1} = 4.2$ wherein the maximum velocity of the oscillator block is very close to the belt velocity for $K_{c1} = 4$ implying that it is at the impending sticking phase.

5   CONCLUSIONS

In this paper, we considered a linear time-delayed position feedback in controlling friction-induced vibrations in a single-degree-of-freedom spring-mass-damper system on a moving belt. A dynamic (LuGre) friction model is considered for the analysis for which the bifurcation is subcritical in nature for the uncontrolled system [20, 16] and consequently, the system is prone to large amplitude vibrations near the stability boundary. We explore the possibility of changing the nature of bifurcation from subcritical to supercritical by applying the control force in a direction normal to the friction force. Linear stability analysis is performed to obtain the critical belt velocity corresponding to the Hopf bifurcation point. The changing nature of bifurcation is verified through bifurcation diagrams of the system obtained numerically using the software package DDE-BIFTOOL. We find a pair of critical belt velocities for a particular set of control parameters signifying stable equilibriums for low and high belt velocities and unstable equilibriums for the intermediate belt velocities. Numerically obtained bifurcation diagrams capture the lower critical belt velocity only when the bifurcation is supercritical in nature. We also find an interesting result in which the unstable pure slipping limit cycle gives birth to a stable pure slipping limit cycle at the turning point (cyclic fold bifurcation point).

REFERENCES

[1] G. Sheng, *Friction-induced Vibrations and Sound: Principles and Applications*. CRC Press, 2008.

[2] H. Hetzler, D. Schwarzer and W. Seemann, Analytical investigation of steady-state stability and Hopf-bifurcations occurring in sliding friction oscillators with application to low-frequency disc brake noise. *Communications in Nonlinear Science and Numerical Simulation*, **12**, 83–99, 2007.

[3] N. Hinrichs, M. Oestreich and K. Popp, On the modeling of friction oscillators. *Journal of Sound and Vibration*, **216**, 435–459, 1998.

[4] J.J. Thomsen, Using fast vibrations to quench friction induced oscillations. *Journal of Sound and Vibration*, **218**, 1079–1102, 1999.

[5] N. Hoffmann, M. Fischer, R. Allgaier and L. Gaul, A minimal model for studying properties of the mode-coupling type instability in friction induced oscillations. *Mechanics research communicaitions*, **29**, 197–205, 2002.

[6] N. Hoffmann and L. Gaul, Effects of damping on mode coupling instability in friction induced oscillations. *ZAMM Zeitschrift fur angewandte Mathematik und Mechanik*, **83**, 524–534, 2003.

[7] R.A. Ibrahim, Friction-induced vibration, chatter, squeal, and chaos: PartII: dynamics and modeling. *ASME Applied Mechanics Review*, **47**, 227–253, 1994.

[8] N. Hoffmann and L. Gaul, A sufficient criterion for the onset of sprag-slip oscillations. *Archive of applied mechanics*, **73**, 650–660, 2004.

[9] A. Ruina, Slip instability and state variable friction laws. *Journal of Geophysical Research*, **88**, 10359–10370, 1983.

[10] C. Canudas de Wit, H. Olsson, K.J. Åström and P. Lischinsky, A new model for control of systems with friction. *IEEE Transactions on Automatic Control*, **40**, 419–425, 1995.

[11] P. Dupont, V. Hayward, B. Armstrong and F. Altpeter, Single state elasto-plastic friction models. *IEEE Transactions on Automatic Control*, **47**, 787–792, 2002.

[12] A.J. McMillan, A non-linear friction model for self-excited vibrations. *Journal of Sound and Vibration*, **205**, 323–335, 1997.

[13] J. Wojewoda, A. Stefanski, M. Weircigroch and T. Kapitaniak, Hysteretic effects of dry friction: modelling and experimental studies. *Philosophical transactions of the royal society A*, **366**, 747–765, 2008.

[14] K. Guo and X. Zhang and H. Li and G. Meng, Non-reversible friction modeling and identification. *Archive of Applied Mechanics*, **78**, 795–809, 2008.

[15] A. Saha, B. Bhattacharya and P. Wahi, A comparative study on the control of friction-driven oscillations by time-delayed feedback. *Nonlinear Dynamics*, **60**, 15–37, 2010.

[16] A. Saha and P. Wahi, Delayed feedback for controlling the nature of bifurcations in friction-induced vibrations. *Journal of Sound and Vibration*, **330**, 6070–6087, 2011.

[17] A. Saha, S.S. Pandey, B. Bhattacharya and P. Wahi, Analysis and control of friction-induced oscillations in a continuous system. *Journal of Vibration and Control*, **18**, 467–480, 2012.

[18] R. Bell and M. Burdekin, A study of the stick-slip motion of machine tool feed drives. *Proceedings of the Institution of Mechanical Engineers*, **184**, 543–560, 1969.

[19] D. P. Hess and A. Soom, Friction at a lubricated line contact operating at oscillating sliding velocities. *Journal of Tribology*, **112**, 147–152, 1990.

[20] A. Saha, *Analysis and control of friction-induced vibrations by time-delayed feedback*. PhD thesis, Indian Institute of Technology, Kanpur, India, 2013.

[21] K. Popp and M. Rudolph, Vibration control to avoid stick-slip motion. *Journal of Vibration and Control*, **10**, 1585–1600, 2004.

[22] J. Das and A.K. Mallik, Control of friction driven oscillation by time-delayed state feedback. *Journal of Sound and Vibration*, **297**, 578–594, 2006.

[23] S. Chatterjee, Time-delayed feedback control of friction-induced instability. *International Journal of Non-Linear Mechanics*, **42**, 1127–1143, 2007.

[24] K. Engelborghs, T. Luzyanina and D. Roose, Numerical bifurcation analysis of delay differential equations using DDE-BIFTOOL. *ACM Transactions on Mathematical Software (TOMS)*, **28**, 1–21, 2002.